water

MDPI

Article

A Study of Hydrogeochemical Processes on Karst Groundwater Using a Mass Balance Model in the Liulin Spring Area, North China

Xiuqing Zheng [1], Hongfei Zang [2], Yongbo Zhang [1,*], Junfeng Chen [1], Fei Zhang [3] and Yu Shen [4]

1 College of Water Resources Science and Engineering, Taiyuan University of Technology, Taiyuan 030024, China; zhengxiuqing@tyut.edu.cn (X.Z.); chenjunfeng@tyut.edu.cn (J.C.)
2 School of Water Conservancy, North China University of Water Resources and Electric Power, Zhengzhou 450046, China; zanghongfei@ncwu.edu.cn
3 Taiyuan Design Research Institute for Coal Industry, Taiyuan 030001, China; zhangfeisxfy@gmail.com
4 Shanxi Hydrology and Water Resources Survey Bureau, Taiyuan 030001, China; shenyuwater@gmail.com
* Correspondence: zhangyongbo@tyut.edu.cn; Tel.: +86-351-611-1150

Received: 13 May 2018; Accepted: 30 June 2018; Published: 10 July 2018

Abstract: Exploring the hydrogeochemical processes of karst groundwater has significant meaning for protecting local groundwater systems in semi-arid areas. Taking a typical semi-arid karst groundwater system—the Liulin spring area—as the research region, hydrogeochemical processes from rainfall infiltration to formation of higher total dissolved solids (TDS) water were studied, applying a mass balance model and the prediction of water chemical components in the focus area was explored. The results showed that hydrogeochemical processes dominating chemical components of karst groundwater included lixiviation, cation exchange and mixture. Calcite dissolved during rainfall infiltration processes in recharge area and saturated, then precipitated along the whole flow path. CO_2 dissolved significantly along with rainfall infiltration process and outgassed in discharge area and stagnant area. The dissolution of dolomite, gypsum and halite accompanied entire flow path and maximum dissolution load occurred in stagnant area. Mg-Na or Ca-Na exchange prevailed along flow path but exchange types depended on ionic concentration. The mixture between surface water and karst groundwater took place in surface water leakage belt in recharge and discharge area and mixture ratio for surface water ranged from 40% to 70%. TDS of the Liulin springs will increase with decreasing surface water leakage. Conversely, TDS of karst groundwater near Henggou area will decrease accompanied by the continuous discharge of the Henggou artesian well.

Keywords: karst groundwater; hydrogeochemical processes; mass balance model; the Liulin spring area

1. Introduction

Karst groundwater, on account of better quality, stable quantity and concentrated discharge by spring, is the major water supply source for industrial, agricultural and residential water uses in semi-arid area in northwest China [1]. Chemical balances of karst groundwater are broken by both natural factors and human activities [2]. Therefore, studying hydrogeochemical processes is essential to explore hydrogeological cycle and to search reasonable exploitation plan of karst groundwater.

The Liulin spring area is a typical karst groundwater system in semi-arid area with dominantly water-bearing medium being karstic fracture and pore [3]. Add up with the complicated regional geologic setting, to study characteristics of karst groundwater system is hard. Most of the previous study were focused on groundwater flow system in this area [4–7]. Recently, the methods for applying hydrogeochemical simulation techniques to researching hydrochemical evolution provided

us with a powerful tool for handling complex hydrogeochemical problems [8–13]. By applying geological statistics, Piper diagrams and hydrogeochemical simulation techniques, Wang et al. [14,15] and Ma et al. [16–18] obtained hydrological information on the surface water and groundwater and depicted karst groundwater chemical characteristics in the Liulin spring area. Zang et al. [19,20] traced the source of major ions in karst groundwater using isotopic tracing techniques and hydrogeochemical methods. There were hardly any studies focused on hydrogeochemical processes of karst groundwater from rainfall infiltration in recharge area to forming higher Total Dissolved Solids (TDS) groundwater in stagnant area.

According to regional hydrologic and hydrogeological conditions and in situ sampling campaign for water chemistry, hydrogeochemical processes are researched using mass balance model and prediction for water chemical components in the focus area were explored.

2. Study Area

The Liulin spring area, with an area of 6080.54 km^2, lies between the Western Shanxi Loess Plateau and the Lvliang Ranges. The study area is subject to continental monsoon climate with a mean annual temperature, rainfall and potential evapotranspiration of 9.2 °C, 508 mm and 1186 mm, respectively. The rainfall in July, August and September represents approximately 66% of the precipitation received in a whole year. The annual mean relative humidity of air is about 54~62% in study area. The Sanchuan River and its tributaries, including the Beichuan River, the Dongchuan River and the Nanchuan River, are the major surface water resources (Figure 1) in study area. The terrain altitude in the east end of the study area is much higher than that of the west end, with elevations of 800 to 2800 m asl (above sea level). The Liulin spring, emerging in spots from the Zhaidong village to the Shangqinglong village in the valley of the Sanchuan River in Liulin County (Figure 1) with elevations of ~792 to 803 m above sea level, consists of the Zhaidong springs group, the Shangqinglong springs group, the Longmenhui springs group, the Yangjiagang springs group and the Liujiageta springs group.

Regular Precambrian metamorphic rock outcroppings can be found in the northern, eastern and southern parts of the spring area, while Cambrian-Ordovician carbonate strata outcroppings are found mostly in the south-eastern and central parts of the spring area (Figure 1). Carboniferous-Triassic clastic rocks are mainly outcropped in the western and central regions of the spring area. Tertiary and Quaternary rickle overlies various ages of the bedrock. From a geotectonic point of view, the spring area is situated in a uniclinal structure which tilts to the west with a 2- to 8-degree dip angle, within which secondary folds and fractures develop. The geologic structure dominates the directions of the groundwater flow.

The northern and eastern boundaries of spring area are composed of drainage divides in metamorphic rocks mountains, whereas the southern and south-eastern boundaries consist of subsurface divides in exposed areas of carbonate rocks. In the western part of the study area, carbonate rocks incline toward the syncline core of the Ordos Basin and are covered by thick-bedded clastic rocks for hundreds of meters and velocity of karst groundwater flow was very slow. This boundary was defined as the lines where the roof depth of carbonate rocks reaches to 1000 m. Cambrian and Ordovician marine carbonate rocks constitute the main aquifer for the water supply, especially the middle series of the Ordovician, which consists of limestone, dolomite and some of gypsum. The upper and the lower confining bed are composed of Carboniferous-Triassic clastic rocks and Precambrian metamorphic rocks, respectively.

The karst groundwater system is mainly recharged in exposed areas of carbonate rocks and these areas were defined as the recharge area. Leakage of river water from the Shanchuan River and its tributaries in exposed areas of carbonate rocks serve as additional recharge sources. In the center of the spring area, carbonate rocks are covered by thick-bedded clastic rocks which are composed of interbed of sandstone and mudstone preventing the precipitation recharging the aquifer. This serves as the flow-through area, with the waters flowing from the north, east and south parts of study area towards the Liulin spring. There are two major discharge ways in this groundwater system: spring discharge

and well exploitation. Places where the springs emerge in the Sanchuan River valley constitute the dominant discharge regions of the groundwater system.

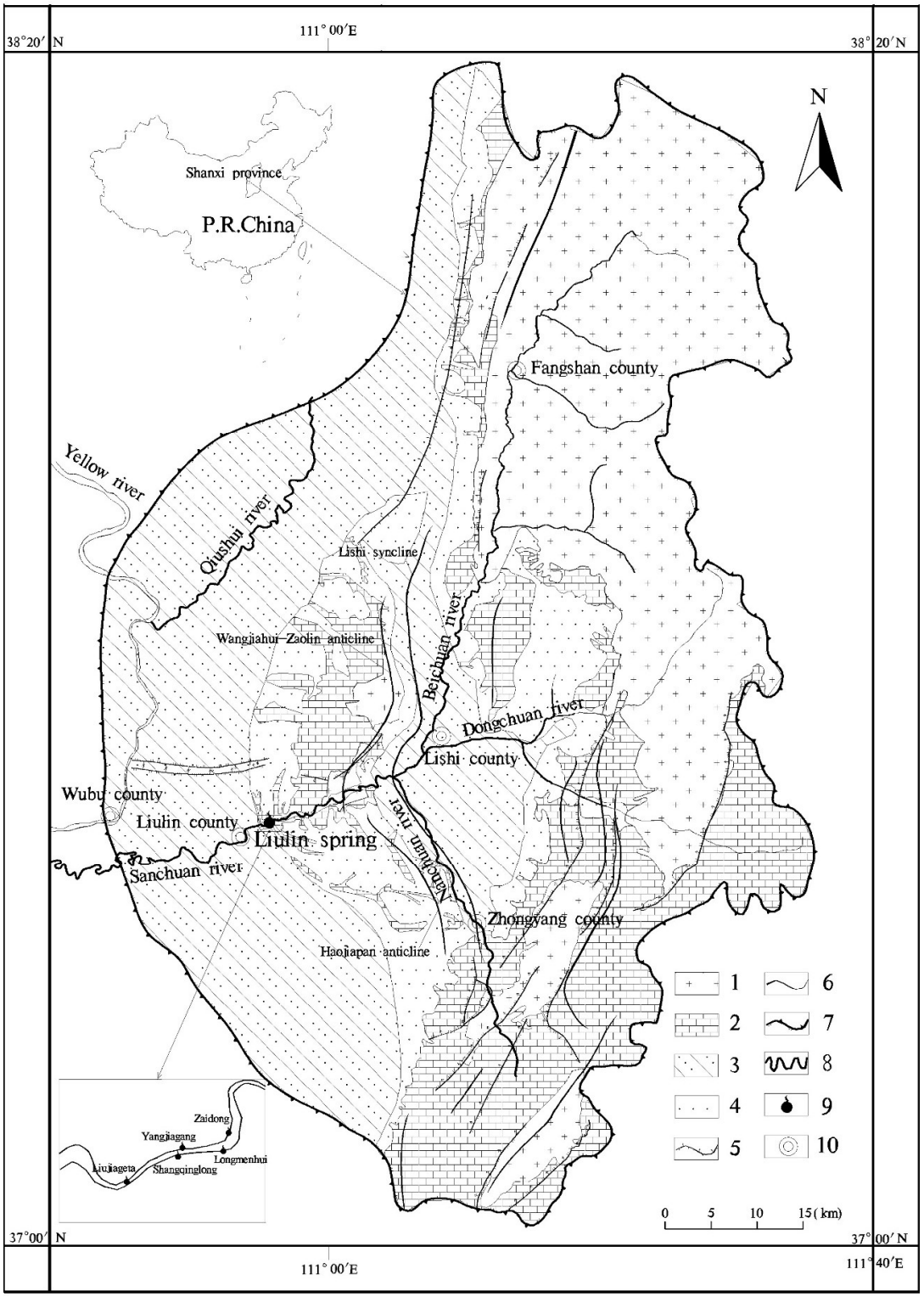

Figure 1. Simplified geological map of Liulin karst water system with an enlarged view of the locations of springs. 1: Precambrian metamorphic rocks; 2: Cambrian and Ordovician carbonate rocks; 3: Carboniferous-Triassic clastic rocks; 4: Neogene-Quaternary rickle; 5: fault; 6: fold; 7: boundary of spring area; 8: river; 9: spring; 10: city.

The average monthly spring discharge over 36 years (from January 1974 to December 2009) was 2.28 m^3/s, with a maximum discharge of 5.62 m^3/s in April 1979 and a minimum discharge of 0.87 m^3/s in October 1984, as shown in Figure 2. The spring discharge decrease continuously from 1979 in which it reached to the maximum value, due to increasing karst groundwater exploitation and decreasing rainfall [2].

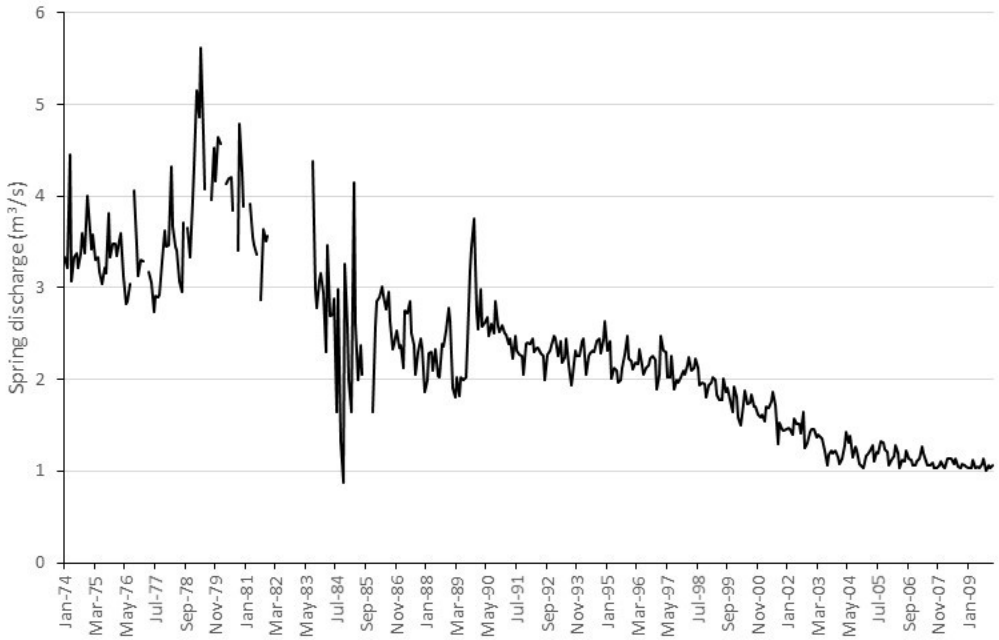

Figure 2. Hydrographs of the spring discharge of the Liulin spring (from January 1974 to December 2009).

3. Methodology

Hydrogeochemical simulation technique, using physic-chemical model and mathematical model, was chosen to depict hydrogeochemical processes of natural water system and water-rock system and to stimulate numerically open geochemical system with multi-variables and multi-components reactions [10]. The essential points followed as: two water sites, named as initial water site and final water site, were defined following the groundwater flow path. The water chemical components of final water could be regarded as these components of initial water reacting with surrounding rocks. The whole process following the mass conservation law which means the total amount of the components were constant. The above process could be described as:

Water chemical components of initial water + reaction phases = water chemical components of final water + product phases.

"reaction phase" and "product phase" represented the water chemical components entering of leaving solution along flow path, respectively. They were both known as mineral phases, could be gas, minerals, ion exchange between solids and solution and so on [9]. The relation stated above could also be represented by the equations following mass conservation and charge conservation:

$$\sum_{p=1}^{P} \alpha_p \mathrm{b}_{p,k} = m_{T,k}(\mathrm{final}) - m_{T,k}(\mathrm{initial}) = \Delta m_{T,k} \ (k = 1, \cdots, J) \quad (1)$$

where P was the total amount of reaction phase and product phase in this reaction; α_p indicated the molar mass of mineral p that entered or left solution, also called mass transport amount; $b_{p,k}$ referred to stoichiometric number of k elements in mineral p; $m_{T,k}$ was total molar concentrations of element k and J indicated the number of elements participating in the chemical reaction [10].

$$\sum_{p=1}^{p} u_p \alpha_p = \sum_{i=1}^{i} u_i m_i(\text{final}) - \sum_{i=1}^{i} u_i m_i(\text{initial}) \quad (2)$$

where u_p was valence of the mineral p; u_i referred to valence of the component i; m_i indicated molar concentrations of the component i; others were the same as above.

The number of reactant phases and product phases could be obtained from the quantities of mass transfer, which could be calculated from Equations (1) and (2). Number of elements in mass balance model may be less than number of mineral phase, which may lead to multiple simulated results. Thus, the simulated results must be verified in combination with regional hydrogeological background, such as characteristics of mineral and deposit sediments, isotopes data, rationality of thermodynamics and so on and this feature was the main disadvantages of mass balance model [10].

Simulation process was generally performed by computer program. Dozens of which, like commonly used MINTEQA2 (Environmental Research Laboratory, Athens, GA, USA), WATEQ4F (U. S. Geological Survey, Reston, VA, USA), PHREEQC (U.S. Geological Survey, Reston, VA, USA), EQ3/6 (Lawrence Livermore National Laboratory, Livermore, CA, USA) and NETPATH (U.S. Geological Survey, Reston, VA, USA), were all served in the hydrogeochemical simulation. NETPATH(2009), developed by USGS, was an interactive Fortran 77 computer program used to interpret net geochemical mass balance reactions between an initial and final water along flow path. NETPATH computed the mixing proportions of two to five initial waters and net geochemical reactions that accounted for the observed composition of a final water [21,22]. Hydrogeochemical processes along flow path will be simulated using NETPATH based on water analysis data sampling in May 2011. The uncertainties of these models are all within 5%.

Based on the results of mass balance simulation, forward model was applied to simulate the evolutionary trends of karst groundwater chemical components. This model could be simulated by EQUILIBRIUM PHASES Block in PHREEQC. The accuracy of simulating results was up to the given reaction conditions, including choice for minerals phase of reactant and setting of constraint conditions which usually comprised by equilibrium constant constraint and reactant quantity constraint.

We should notice that, in contrast with solute transport model of groundwater flow, the hydrodynamic dispersion of water chemical compositions and its temporal variation was not considered in the mass balance model and only major ionic concentrations were simulated. Thus, the error may exist, especially for the karat groundwater with higher TDS, this error may be higher. For forward model, the results relied heavily on setting conditions. Thus, to get a reliable result, reacting conditions must be reflected actual situation as much as possible. Considering complexity of hydrogeochemical processes and karst groundwater aquifer, the results simulated above could be just a possibility for water environment evolution.

4. Sampling and Analysis

Sample collection and component analysis of the groundwater is the basis of the following hydrogeochemical evolution analysis and simulation. The precision of which may directly influence reliability and rationality of the simulated results. The groundwater samples numbered from NO01 to NO10 were collected along predominant groundwater flow path in May 2011 (Figure 3). The testing of water chemical components including temperature, pH value, Eh value, HCO_3^-, SO_4^{2-}, Cl^-, Na^+, Ca^{2+}, Mg^{2+} and TDS was accomplished in water environmental monitoring center of Shanxi province. Precipitation sample (NO11) was collected by Lishi meteorological station in May 2009. For lack of temperature data in precipitation, the mean annual temperature of spring area was adopted. The surface water data from the research conducted by Wang et al. [15] in 1995 was employed in the simulation process. Meanwhile, water chemical analysis data (NO13) was collected in 1979 of Henggou1# to present mixture of karst groundwater in stagnant area.

Temperature, pH value and Oxidation-Reduction Potential (ORP) value were measured in situ using potable REX PHB-4 pH meters and 501 ORP pole. Water sample for cation and anion analysis

were filtered through 0.45 μm membranes in the field and collected in 500 mL polyethylene bottles. HCO_3^- was measured using the Gran titration method [23] in the sampling day. Samples for cation analysis were acidified using 1:1 nitric acid to pH < 2 in field. The cations (Na^+, Ca^{2+}, Mg^{2+}) and anions (Cl^-, SO_4^{2-}) were determined by atomic absorption spectrometry (TAS990F, Persee, Beijing, China) and ion chromatography (CIC300, Shenghan, Qingdao, China), respectively. The uncertainties of measurements were all within 5%. The results were given in Table 1.

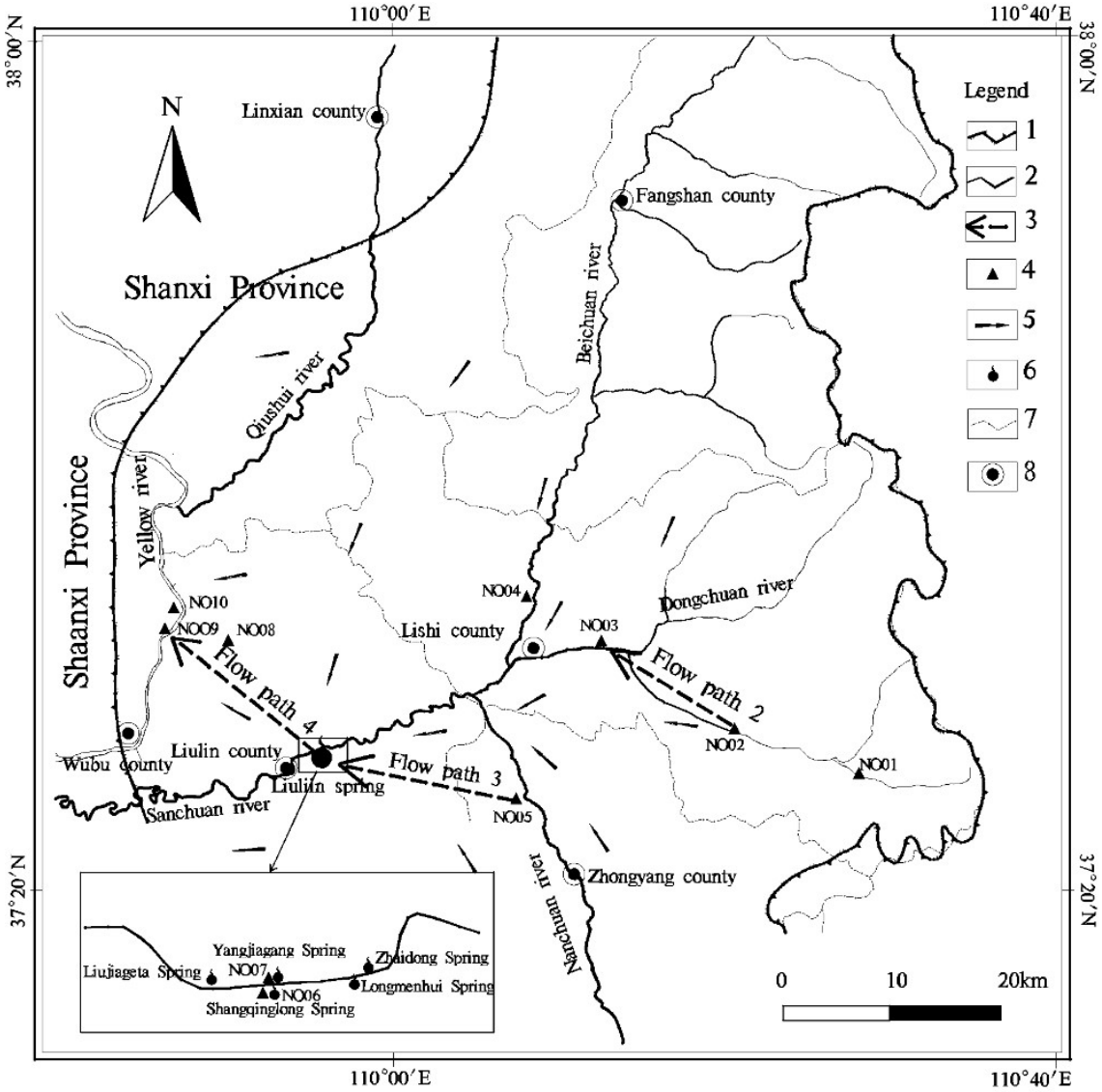

Figure 3. Map of study area showing the sampling sites. 1: boundary of spring area; 2: river system; 3: the selected flow path for simulation; 4: sampling sites of water quality; 5: flow directions of karst groundwater; 6: springs; 7: county boundary; 8: City.

Table 1. Physico-chemical data of water samples in Liulin spring area mg/L.

NO.	Sampling Sites	Year	Water Types	Sub-Region	T (°C)	Eh (pV)	pH	Na^+	Ca^{2+}	Mg^{2+}	Cl^-	$SO_4{}^{2-}$	$HCO_3{}^-$
NO01	Wucheng	2011	Karst groundwater	Recharge area	12.00	2.74	7.66	11.3	62.1	19.4	6.03	29.8	277
NO02	Youfangping	2011	Karst groundwater	Recharge area	11.00	2.77	7.78	18.4	64.5	19.9	10.6	43.2	278
NO03	Tianjiahui	2011	Karst groundwater	Flow-through area	17.00	2.08	7.93	41.2	60.5	17.7	36.2	35.5	277
NO04	Shangan	2011	Karst groundwater	Flow-through area	11.50	4.09	7.58	49.2	66.9	25.8	31.2	86.5	277
NO05	Jinluo	2011	Karst groundwater	Flow-through area	16.00	2.11	7.54	41.5	57.3	43	3.54	113	271
NO06	Shangqinglong	2011	Karst groundwater	Discharge area	16.00	2.86	7.63	81.5	66.9	24.8	51.8	90.3	271
NO07	Yangjiagang	2011	Karst groundwater	Discharge area	15.00	2.75	7.6	174	123	27.2	172	280	320
NO08	Baijiayan	2011	Karst groundwater	Stagnant area	22.50	1.20	7.19	445	180	69.3	568	377	303
NO09	Henggou1#	2011	Karst groundwater	Stagnant area	33.00	−4.88	6.84	2240	749	190	3550	1780	235
NO10	Henggou2#	2011	Karst groundwater	Stagnant area	35.00	−4.43	6.93	1760	552	229	2720	1640	246
NO11	Lishi meteorological station	2009	Precipitation	-	10	4.00	7.1	4.4	6.5	2.0	1.5	10.4	25.1
NO12	Sanchuan River	1995	Surfaces water	-	21.8	4.00	6.8	11.1	41.0	12.8	9.3	30.4	174.2
NO13	Hengou 1#	1979	Karst groundwater	Stagnant area	36.0	-	-	3030	1057	260	4893	2698	212

5. Results and Discussion

5.1. Water Chemical Characteristics

The temperature of karst groundwater generally increased along flow path with a range of 11.5 to 35 centigrade. Variation range of pH values were located between 6.8 and 8.2 with a mean value of 7.5, all of which situated in normal range (6.5~8.5) of groundwater. The redox potential (pE values) varied from −4.88 to 4.09 with a mean value of 1.13. Not significantly different mean pE values of 2.75, 2.76 and 2.81 in recharge area, flow-through area and discharge area respectively indicated an oxidation environment in the karst groundwater in these areas. The Mean values of pE in stagnant area were relatively low, some even negative in west boundary of spring area, indicating that redox state of karst groundwater transferred from oxidation environment to reduction environment. The concentrations of major anions and cations of karst groundwater varied dramatically, which contributed by local geological conditions and karst groundwater regime. The ranges of concentrations of Cl^-, SO_4^{2-}, HCO_3^-, Na^+, Ca^{2+} and Mg^{2+} were 4~3550 mg/L, 30~1780 mg/L, 235~320 mg/L, 11~2240 mg/L, 57~749 mg/L and 18~229 mg/L, respectively, with a mean value of 715 mg/L, 448 mg/L, 276 mg/L, 486 mg/L, 198 mg/L and 67 mg/L. Almost all the major ionic concentrations increased along flow path except that of HCO_3^- with relatively small variation.

5.2. Inverse Hydrogeochemical Simulation

5.2.1. Choice of Simulation Path

To establish an inverse hydrogeochemical models, flow paths must be chosen firstly. The variation of mineral phase, water chemical and spatial distribution of various ions must be considered in this process [10]. Four flow paths were determined:

Flow path1: Precipitation → Youfangping
Flow path2: Youfangping + Surface water → Tianjiahui
Flow path3: Jinluo + Surface water→ Shangqinglong
Flow path4: Yangjiagang + Henggou1#(1979) → Henggou1#(2011)

Hydrogeochemical processes were simulated through flow path 1 to 3 representing precipitation infiltration, recharge area to flow-through area and flow-through area to discharge area respectively, as was shown in Figure 3. The surface water leakage was considered in path 2 and 3. Total Dissolved Solids (TDS) and major ionic concentrations of karst groundwater in Henggou1# artesian well decreased continuously since its excavating [2], which may have resulted from capturing of karst groundwater with low ionic concentrations in discharge area. Thus, current karst groundwater near Henggou could be regarded as the water in 1979, excavating year of Henggou1#, mixed with that in discharge area, which was flow path 4 refer to.

5.2.2. Determination of Mineral Phases

Selecting mineral phases, which based on lithology, mineral constituent and aquifer characteristics, was crucial to establish mass balance model. According to local hydrogeological conditions, lithology and mineral saturation index of karst groundwater [19], calcite, dolomite, gypsum and halite were selected. Meanwhile, CO_2 (gas), Ca-Na and Mg-Na ion exchange were also taken as input phases of the model. Constrained by crystallization kinetics, it was hard to meet primary dolomite under modern sedimentary environment and hard to synthesize dolomite in laboratory under the surface temperature and pressure [24]. Thus, dolomite was dissolved only in the model.

5.2.3. Establishment of Simulation Model

According to the selected mineral phases, the main elements in the model were Ca, Mg, C, S, Na and Cl and the mass balance model was:

$$\begin{cases} CaCO_3(\text{Calcite}) + CaMg(CO_3)_2(\text{Dolomite}) + CaSO_4{\cdot}nH_2O(\text{Gypsum}) \\ +CaX(\text{Cation} - \text{exchange material}) = \Delta m_{T,\text{Ca}} \\ CaMg(CO_3)_2(\text{Dolomite}) + MgX(\text{Cation} - \text{exchange material}) = \Delta m_{T,\text{Mg}} \\ CaCO_3(\text{Calcite}) + 2CaMg(CO_3)_2(\text{Dolomite}) + CO_2(\text{g}) = \Delta m_{T,\text{C}} \\ CaSO_4{\cdot}nH_2O(\text{Gypsum}) = \Delta m_{T,\text{S}} \\ 2CaX(\text{or } 2MgX)(\text{Cation} - \text{exchange material}) + NaCl(\text{Halite}) = \Delta m_{T,\text{Na}} \\ NaCl(\text{Halite}) = \Delta m_{T,\text{Cl}} \end{cases}$$

where $\Delta m_{T,A}$ was total molar mass of A element.

5.2.4. Modeling Results and Discussion

By importing initial water, final water, mineral phases and other input items into NETPATH, the simulating results of hydrogeochemical processes were provided and shown in Table 2.

(1) Flow path 1

Dissolved and precipitated amounts of mineral phases along flow path 1 were shown in Table 1. Two qualified models were found by NETPATH. Calcite, dolomite, gypsum, halite and CO_2 (g) dissolved significantly during rainfall infiltration, with remarkable Ca-Na or Mg-Na exchange. The dissolved concentration of CO_2 (g) in groundwater (2.85 mmol/L) was the highest one followed by which of dolomite (1.08 mmol/L), the same index of other minerals was relatively small. Cation exchange was dominated by Mg-Na exchange, that was Mg^{2+} leaving solution and Na^+ entering solution by ion-exchange adsorption. The same dissolved concentrations of gypsum, halite and CO_2 (g) were kept in model 2 as in model 1, of which decreased in dolomite and increased in calcite. Meanwhile, the cation exchange changed to Ca-Na in model 2 instead of Mg-Na in model 1 with the same exchange quantities. Both the models could well explain hydrogeochemical processes along flow path 1. Model 2 was considered more reasonable in Liulin spring area for calcite had a greater dissolved rate than dolomite [25] and Ca^{2+} possessed a greater molar concentration and exchange capacity.

(2) Flow path 2

Concentration changes of mineral phases in groundwater along flow path 2 were shown in Table 2. NETPATH solved four models meeting constraints. In model 1, the largest dissolved mineral was halite, followed by dolomite. The amount of CO_2 outgas was 0.04 mmol/L. Mg-Na exchange was the principle cation exchange with secondary Ca-Na ion exchange, that was Ca^{2+} and Mg^{2+} leaving solution by absorption and Na^+ entering solution by exchange. Calcite and gypsum were absent in this model. The most dissolved mineral in model 2 still be halite and then to dolomite and little gypsum. Major cation exchange was Mg-Na exchange yet, while calcite and CO_2 do not incorporate in the processes. In model 3, calcite precipitated and CO_2 outgassed, while halite and dolomite still dissolved, accompanying Mg-Na exchange. Hydrogeochemical processes in model 4 shown dissolution of halite, gypsum and dolomite, precipitation of calcite and Mg-Na exchange. All of the four models could better explain hydrogeochemical processes along flow path 1. The research [19] for SI (saturated index) for sample NO3 indicated that the SI of calcite and gypsum was 0.63 and −2.1, respectively, suggesting precipitation of calcite and dissolution of gypsum. Thus, model 4 may be more realistic in this region. Mixture of surface water and groundwater occurred during groundwater flow from recharge area to flow-through area with a ratio about 3:1.

Table 2. Simulating results for inverse model.

NO.	Models	Mixture Proportion		Transferring Molar Concentration of Mineral Phases (mmol/L)							
				Calcite	Dolomite	Gypsum	Halite	CO_2(g)	CaX_2	MgX_2	NaX
The flow path 1	Model 1	/	/	0.26	1.02	0.31	0.25	2.85	/	−0.21	0.42
	Model 2	/	/	0.68	0.81	0.31	0.25	2.85	−0.21	/	0.42
The flow path 2	Model 1	0.51	0.49	/	0.22	/	0.70	−0.04	−0.06	−0.19	0.50
	Model 2	0.27	0.73	/	0.34	0.03	0.71	/	−0.06	−0.23	0.57
	Model 3	0.51	0.49	−0.12	0.29	/	0.70	−0.04	/	−0.25	0.50
	Model 4	0.27	0.73	−0.12	0.40	0.03	0.71	/	/	−0.28	0.57
The flow path 3	Model 1	0.58	0.42	/	0.23	0.14	1.31	−0.08	/	−0.48	0.97
	Model 2	0.58	0.42	/	0.23	0.14	1.31	/	/	−0.48	0.97
	Model 3	0.00	1.00	/	0.61	0.66	1.22	−0.21	−0.72	−0.17	1.79
The flow path 4	Model 1	0.87	0.13	−0.59	/	12.68	82.67	−0.41	0.29	5.55	−11.68
	Model 2	0.87	0.13	−11.68	5.55	12.68	82.67	−0.41	5.84	/	−11.68

Notes: Positive means dissolution and negative indicates precipitation; NaX is molar mass of Na^+ entering solution via cation exchange.

(3) Flow path 3

The results of dissolution and precipitation of mineral phases for flow path 3 were listed in Table 2. Three models satisfying constraints were solved by NETPATH. In model 1, the largest amount of dissolved minerals in groundwater was halite (1.31 mmol/L), followed by dolomite (1.08 mmol/L), accompanying CO_2 outgassing (0.08 mmol/L) and Mg-Na cation exchange. Calcite did not occur in model 1, indicating that this mineral may be in a balance state. Model 2 shown a similar process as model 1, only different was the absent of CO_2 which indicated that it kept balanced during the process. In model 3, halite, gypsum and dolomite dissolved with CO_2 outgassing and cation exchange was dominated by Ca-Na exchange with minor Mg-Na exchange. Calcite did not show up in this model too. Model 3 does not meet physical condition of spring area because mixture ratio for groundwater was zero, which meant that karst groundwater of sample NO05 just derived from surface water rather than groundwater flow from flow-through area. The evidence of sinter [2] near springs indicated that CO_2 was outgassing through the processes which makes model 1 more qualified with the real condition. The surface water and groundwater mixed from flow-through area to discharge area with percentages of 42% and 58% respectively.

(4) Flow path 4

There were 2 models along flow path 4 found by NETPATH, as shown in Table 2. Generally speaking, gypsum and halite dissolved remarkably along this flow path and CO_2 outgassed. For ion exchange, Na^+ left solution by absorption and Ca^{2+} and Mg^{2+} entered solution by exchange. The mixture ratio between the cold water (NO07) and thermal water (NO13) was about 7:1. In model 1, calcite precipitated slightly, while dolomite did not participate in. Nevertheless, calcite precipitated significantly with remarkable dolomite dissolution in model 2. For common ion effect, calcite precipitated resulting from significant dissolution of gypsum. Furthermore, precipitation of calcite could take away some HCO_3^-, then caused to dissolution of dolomite, which was so-called dedolomitization [26–28]. Thus, model 2 may be the better one in Liulin spring area.

According to simulated results stated above, hydrogeochemical processes controlling karst groundwater chemical components consisted of lixiviation (dissolution and precipitation of mineral, dissolution and outgassing of gases), cation exchange, mixture and so on. Various sub-region corresponded with different dominant hydrogeochemical processes. These results were coincided with the results studied by Wang [15] and Zang [19].

Calcite dissolved mainly during rainfall infiltration in recharge area, saturated after the infiltration and precipitated during groundwater flow from recharge area to stagnant area. CO_2 dissolved significantly accompanying rainfall infiltration and outgassed in discharge area and stagnant area. Dolomite, gypsum and halite dissolved all along flow path, while the maximum amount of dissolution occurred in stagnant area. Mg-Na or Ca-Na exchange also occurred along entire flow path. However, the types of cation exchange varied according to ionic concentration in different areas. The mixture of surface water and karst groundwater took place in surface water leakage belt in recharge area and near up-gradient of Liulin spring and mixture ratio for surface water ranged from 40% to 70%. In particular, for without considering hydrodynamic dispersion of groundwater components in simulation processes and just considering concentration of macro components, there may be a certain error or inaccuracy for simulated results, especially for karst groundwater with higher TDS and ionic strength.

What is more, according to regional formation lithology, mineral and hydrogeological conditions, redox, which was exclude in the simulated model and confirmed by a smell of H_2S in sampling campaign in Henggou, may influenced chemical components of karst groundwater, which should be further studied.

5.3. The Evolutionary Trends of Karst Groundwater Chemical Components in Focal Area

In the Liulin spring area, variation of groundwater chemical components and discharge of the Liulin springs and the influence of Henggou artesian well on karst groundwater system were the focus

between the government and people. Thus, this research will explore evolutionary trends of karst groundwater chemical components in these two areas.

5.3.1. The Effect of Decreased Surface Leakage on Water Chemical Components in Liulin Springs

As stated above, during karst groundwater flowing from runoff area to discharge area, the mixture between surface water and karst groundwater occurred in leakage regions of Sanchuan River near the upgradient of Liulin springs. This mixture could be considered as dilution processes of karst groundwater because of lower ionic content of surface water, resulting in some of ion concentrations (such as SO_4^{2-}) of karst groundwater in Liulin springs less than that in runoff area. Under conditions of human activities, such as construction of reservoir, runoff volume of Sanchuan River decreased, accompanied by decreasing surface water leakage. Supposing an extreme scenario, where the surface leakage decreased to 0, the variation of water chemical components was explored using the forward model. The sample NO05 was selected as initial water. Mineral phases include calcite, dolomite, gypsum and halite. The SI (saturation index), selecting values of karst groundwater for Shangqinglong spring in 2011, was applied to constrain dissolution of calcite and dolomite. Dissolution of gypsum and halite were constrained by transfer amounts simulated by inverse model. Simulated results were shown in Table 3.

Under the setting conditions, almost all the major ion concentrations increased to some extent except Mg^{2+}. The maximum increasing rate for ions was concentrations of Cl^-, up to 318%; next to $Na^+ + K^+$ with 120%. The increase rate of HCO_3^- is insignificant, only 8%. Thus, TDS of karst groundwater will become increasingly higher along with decreasing surface water leakage.

Table 3. Prediction of chemical components in karst groundwater in focal area (mmol/L).

Components	Shangqinglong			Henggou		
	Observed Value	Prediction Value	Increasing Rate (%)	Observed Value	Prediction Value	Increasing Rate (%)
HCO_3^-	5.418	5.854	8%	4.74	6.57	39%
Ca^{2+}	1.670	2.553	53%	18.85	7.88	−58%
Cl^-	1.462	6.108	318%	101.00	87.49	−13%
Mg^{2+}	1.021	0.891	−13%	7.88	8.84	12%
$Na^+ + K^+$	3.547	7.815	120%	98.29	90.21	−8%
SO_4^{2-}	0.941	1.312	40%	18.69	15.59	−17%

Notes: Positive value means increasing, while negative value indicates decreasing.

5.3.2. The Effect of Henggou Artesian Well on Karst Groundwater System

A mixture ratio of "old water" (karst groundwater of the artesian well in 1979) and "new water" (water sample for Yangjiagang) was 1:7 near Henggou according to inverse modeling. By setting the ratio of "new" water to 100%, the forward model was employed to predict the variation trend of major ions concentrations. Mineral phases participating in this process still selected calcite, dolomite, gypsum and halite. The SI values of karst groundwater in Henggou in 2011 was applied to constrain dissolution of calcite and dolomite. Dissolution of gypsum and halite were constrained by transfer amounts simulated by inverse model. Simulated results were shown in Table 3.

The concentration of HCO_3^- and Mg^{2+} increased under setting conditions while concentrations of other ions decreased. A decreasing ratio of 58% occurred in Ca^{2+}, which is the maximum ratio; next was SO_4^{2-} of a ratio of 17%. Thus, TDS of karst groundwater will decrease continuously along with artesian well discharge.

6. Conclusions

1. Dissolution of Calcite mainly occurred during rainfall infiltration processes in the recharge area and precipitated along the whole flow path. While the dissolution of dolomite, gypsum and halite accompanied entire flow path and maximum dissolution load occurred in stagnant area.
2. Results simulated by forward model showed that TDS of the Liulin springs will increase along with decreasing surface water leakage, while these value for karst groundwater near Henggou area will decrease accompanying by continuous discharge of the Henggou artesian well.
3. This paper focus on spatial variation of major ionic concentrations. The temporal variation of ionic concentration need further study.

Author Contributions: X.Z. and Y.Z. designed sampling campaign, analyzed sampling results and wrote the manuscript; H.Z. and F.Z. simulated the mass balance model and plotted the artworks; J.C. carried out sampling campaign; Y.S. assisted with data collections and technical support.

Funding: This research was financially supported by National Natural Science Foundation of China (41572221, 41572239) and Programs from Shanxi Hydrology and Water Resources Survey Bureau (ZNGZ2015-36).

Acknowledgments: The work was supported by Lvliang Municipal Water Management Committee Office, Lvliang, Shanxi Province, China. The authors would like to thank Wang Guoqing and Xing Shuyan for their help on hydrochemical sampling campaigns, data collections and technical support.

Conflicts of Interest: The authors declare no conflicts of interest.

References

1. Han, X.R. *Karst Hydrogeology*; Geological Publishing House: Beijing, China, 2015. (In Chinese)
2. Zheng, X.Q. *An Investigation Report for Impact of Hengou Artesian Well in Wubu County on Liulin Springs*; Taiyuan University of Technology: Taiyuan, China, 2012. (In Chinese)
3. Gao, B.P.; Liang, Y.P.; Wang, W.T. Features of karst water and geologic background in Liulin spring basin. *Carsol. Sin.* **2008**, *27*, 209–214. (In Chinese)
4. Wu, J.C.; Xue, Y.Q.; Huang, H.; Zhang, Z.Z.; Wang, Y.H. Three dimensional numerical simulation for solute transport in fracture-developed area in Liulin Springs, Shanxi Province. *J. Nanjing. Univ. (Nat. Sci.)* **2000**, *36*, 728–734. (In Chinese)
5. Wu, J.C.; Xue, Y.Q.; Huang, H.; Zhang, Z.Z. Two dimensional numerical simulation of solute transport in Liulin spring local area. *J. Hydraul. Eng.* **2001**, *32*, 38–43. (In Chinese)
6. Wu, J.C.; Xue, Y.Q.; Huang, H.; Zhang, Z.Z.; Wang, Y.H. Karst groundwater simulation of Liulin spring area, Shanxi province. *Hydrogeol. Eng. Geol.* **2001**, *28*, 18–20. (In Chinese)
7. Hou, G.C.; Zhang, M.S. *Groundwater Exploration in the Ordos Basin*; Geology Publishing House: Beijing, China, 2001. (In Chinese)
8. Plummer, L.N.; Busby, J.F.; Lee, R.W.; Hanshaw, B.B. Geochemical modeling of the Madison Aquifer in parts of Montana, Wyoming and South Dakota. *Water Resour. Res.* **1990**, *26*, 1981–2014. [CrossRef]
9. Marfia, A.M.; Krishnamurthy, R.V.; Atekwana, E.A.; Panton, W.F. Isotopic and geochemical evolution of ground and surface waters in a karst dominated geological setting: A case study from Belize, Central America. *Appl. Geochem.* **2004**, *19*, 937–946. [CrossRef]
10. Merkel, B.J.; Friedrich, B.P. *Groundwater Geochemistry—A Practical Guide to Modeling of Natural and Contaminated Aquatic Systems*; Springer: Berlin, Germany, 2005.
11. Moral, F.; Cruz-Sanjulian, J.J.; Olias, M. Geochemical evolution of groundwater in the carbonate aquifers of Sierra de Segura (Betic Cordillera, southern Spain). *J. Hydrol.* **2008**, *360*, 281–296. [CrossRef]
12. Ahmed, A.; Clark, I. Groundwater flow and geochemical evolution in the Central Flinders Ranges, South Australia. *SciI. Total Environ.* **2016**, *572*, 837–851. [CrossRef] [PubMed]
13. Gastmans, D.; Hutcheon, I.; Menegario, A.A.; Chang, H.K. Geochemical evolution of groundwater in a basaltic aquifer based on chemical and stable isotopic data: Case study from the Northeastern portion of Serra Geral Aquifer, São Paulo state (Brazil). *J. Hydrol.* **2016**, *535*, 598–611. [CrossRef]
14. Wang, Y.X.; Ma, T.; Luo, C.H.; Li, Y.M. Geochemical modeling of water-rock interactions in the Liulin karst system, Shanxi province. *Earth Sci. J. China Univ. Geosci.* **1998**, *23*, 519–522. (In Chinese)

15. Wang, Y.X.; Ma, T.; Luo, C.H. Geostatistical and geochemical analysis of surface water leakage into groundwater on a regional scale: A case study in the Liulin karst system, northwestern China. *J. Hydrol.* **2001**, *246*, 223–234. [CrossRef]
16. Ma, T.; Wang, Y.X.; Zhang, Q.B. A grey system approach to prediction of surface runoff leakage: With a example from the Liulin karst water system in Shanxi province. *Earth Sci. J. China Univ. Geosci.* **1997**, *22*, 90–93. (In Chinese)
17. Ma, T.; Wang, Y.X. The analysis of water chemical information of groundwater using factor and Kriging analysis in the Liulin spring area in Shanxi province. *Hydrogeol. Eng. Geol.* **1999**, *42*, 44–46. (In Chinese)
18. Ma, T.; Wang, Y.X.; Guo, Q.H.; Zheng, H. Hydrochemical and isotopic evidence of origin of thermal karst water at Taiyuan, northern China. *J. Earth Sci.* **2009**, *20*, 879–889. [CrossRef]
19. Zang, H.F.; Zheng, X.Q.; Jia, Z.X.; Chen, J.F.; Qin, Z.D. The impact of hydrogeochemical processes on karst groundwater quality in arid and semiarid area: A case study in the Liulin spring area, north China. *Arab. J. Geosci.* **2015**, *8*, 6507–6519. [CrossRef]
20. Zang, H.F.; Zheng, X.Q.; Qin, Z.D.; Jia, Z.X. A study of the characteristics of karst groundwater circulation based on multi-isotope approach in the Liulin spring area, North China. *Isot. Environ. Healt Stud.* **2015**, *51*, 271–284. [CrossRef] [PubMed]
21. Plummer, L.N.; Prestemon, E.C.; Parkhurst, D.L. *An Interactive Code (NETPATH) for Modeling Net Geochemical Reactions along a Flow Path*; Water-Resources Investigations Report 94-4169; U.S. Geological Survey: Reston, VA, USA, 1994.
22. El-Kadi, I.A.; Plummer, L.N.; Aggarwal, P. NETPATH-WIN: An interactive user version of the mass-balance model, NETPATH. *Groundwater* **2011**, *49*, 593–599. [CrossRef] [PubMed]
23. Gran, G. Determination of the equivalence point in potentiometric titrations. *Analyst* **1952**, *77*, 661–671. [CrossRef]
24. Zhang, X.F.; Hu, W.X.; Zhang, J.T. Critical problems for dolomite formation and dolomitization models. *Geol. Sci. Technol. Inf.* **2006**, *25*, 32–40. (In Chinese)
25. Liu, Z.H.; Dreybrodt, W.; Li, H.J. Comparison of dissolution rate-determining mechanisms between limestone and dolomite. *Earth Sci. J. China Univ. Geosci.* **2006**, *31*, 411–416. (In Chinese)
26. Back, W.; Hanshaw, B.B.; Plummer, L.N.; Rahn, P.H.; Rightmire, C.T.; Rubin, M. Process and rate of dedolomitization: Mass transfer and ^{14}C dating in a regional carbonate aquifer. *Geol. Soc. Am. Bull.* **1983**, *94*, 1415–1429. [CrossRef]
27. Hanshaw, B.B.; Back, W. Major geochemical processes in the evolution of carbonate-aquifer systems. *J. Hydrol.* **1979**, *43*, 287–312. [CrossRef]
28. Lopez, C.M.; Bouamama, M.; Vallejos, A.; Pulido, B.A. Factors which determine the hydrogeochemical behaviour of karstic springs. A case study from the Betic Cordilleras, Spain. *Appl. Geochem.* **2001**, *16*, 1179–1192. [CrossRef]